

# UC San Diego

## UC San Diego Previously Published Works

### Title

Site-Specific and Enzymatic Cross-Linking of sgRNA Enables Wavelength-Selectable Photoactivated Control of CRISPR Gene Editing

### Permalink

<https://escholarship.org/uc/item/8sh2k9v8>

### Journal

Journal of the American Chemical Society, 144(10)

### ISSN

0002-7863

### Authors

Zhang, Dongyang  
Liu, Luping  
Jin, Shuaijiang  
et al.

### Publication Date

2022-03-16

### DOI

10.1021/jacs.1c12166

Peer reviewed



Published in final edited form as:

*J Am Chem Soc.* 2022 March 16; 144(10): 4487–4495. doi:10.1021/jacs.1c12166.

## Site-specific and enzymatic cross-linking of sgRNA enables wavelength-selectable photo-activated control of CRISPR gene editing

Dongyang Zhang<sup>†</sup>, Luping Liu<sup>†</sup>, Shuaijiang Jin<sup>†</sup>, Ember Tota<sup>†</sup>, Zijie Li<sup>†</sup>, Xijun Piao<sup>†</sup>, Xuan Zhang<sup>‡</sup>, Xiang-Dong Fu<sup>‡</sup>, Neal K. Devaraj<sup>†</sup>

<sup>†</sup>Department of Chemistry and Biochemistry, University of California, San Diego, La Jolla, CA 92093, USA

<sup>‡</sup>Department of Cellular and Molecular Medicine, University of California, San Diego, La Jolla, CA 92093, USA

### Abstract

Chemical cross-linking enables rapid identification of RNA-protein and RNA-nucleic acid inter- and intramolecular interactions. However, no method exists to site-specifically and covalently cross-link two user-defined sites within an RNA. Here, we develop RNA-CLAMP, which enables site-specific and enzymatic cross-linking (clamping) of two selected guanine residues within an RNA. Intramolecular clamping can disrupt normal RNA function, whereas subsequent photocleavage of the crosslinker restores activity. We used RNA-CLAMP to clamp two stem loops within the single-guide RNA (sgRNA) of the CRISPR-Cas9 gene editing system via a photocleavable cross-linker, completely inhibiting editing. Visible light irradiation cleaved the crosslinker and restored gene editing with high spatiotemporal resolution. Design of two photocleavable linkers responsive to different wavelengths of light allowed multiplexed photo-activation of gene editing in mammalian cells. This photo-activated CRISPR-Cas9 gene editing platform benefits from undetectable background activity, provides a choice of activation wavelengths, and has multiplexing capabilities.

### INTRODUCTION

Numerous approaches have been developed to study and control RNA function. RNA probes often rely on non-covalent interactions, as in anti-sense DNA oligos, MS2-tagging, or RNA aptamers.<sup>1–4</sup> Covalent RNA modification strategies offer an additional level of robustness, which can be critical for analyzing or manipulating less abundant RNAs, especially in harsh cellular conditions. However, due to the complex structure and relative instability of RNA, site-specific and covalent modification of RNA remains challenging.<sup>5–7</sup> Chemical cross-linking enables rapid identification of RNA-small molecule, RNA-protein and RNA-

ndevaraj@ucsd.edu .

Supporting Information Available

• Supporting information (additional experimental details, materials, and methods; sequence for all sgRNAs; NMR spectra; HRMS spectra)

nucleic acid inter- and intramolecular interactions, as well as structural studies of complex RNAs.<sup>8–14</sup> However, to date, no method exists to achieve site-specific and covalent cross-linking of two user-defined sites within an RNA of interest. Many RNAs, such as the single-guide RNA (sgRNA) of the CRISPR gene editing system, require secondary and tertiary structure for function, indicating that site-specific cross-linking of two internal nucleotides within an RNA of interest would be useful for studying and manipulating RNA function. Here, we report an RNA-modifying technique, termed RNA-CLAMP, which allows for post-transcriptional and site-specific cross-linking of two guanine nucleotides within a single RNA of interest through a one-step enzymatic process. We applied the RNA-CLAMP technique to the sgRNA of CRISPR-Cas9 system and achieved optical control of gene editing in mammalian cells with high spatiotemporal resolution and multiplexing capability.

Conditionally activated CRISPR-Cas9 gene editing systems allow for greater gene editing precision by limiting Cas9-mediated DNA cleavage to a specific time and location.<sup>15–19</sup> Optical control of CRISPR-Cas9 offers non-invasive manipulation of gene editing with high spatiotemporal resolution by controlling gene editing at a confined location and/or time. Several approaches have been developed to optically control CRISPR-Cas9 gene editing by modifying either the Cas9 protein or the gRNA. For example, a genetically encoded light-activated Cas9 has caged lysine amino acids encoded within the Cas9 protein,<sup>20</sup> and split Cas9 proteins have been fused to a pair of photo-dimerizing proteins to allow optical control of CRISPR-Cas9 gene editing.<sup>21</sup> However, these approaches can suffer from incomplete caging and compromised activity when uncaged. Optical control via the gRNA includes, for example, using photocleavable DNA oligonucleotides that are complementary to the 20-nt target region of the gRNA to block binding to the target DNA.<sup>22</sup> Other gRNA caging strategies include the use of photosensitive small-molecules to mask the RNA, for example, at the 2-OH group or the phosphate backbone of the RNA molecule.<sup>23,24</sup> The caged gRNA can be released upon photocleavage of the protector DNA oligo, resulting in activation of gene editing.<sup>22</sup> However, toxic UV light had to be applied to cells during activation to release the chemical linker used to synthesize the protector DNA oligo. Caged gRNA has been generated by substituting four nucleobases within the 5-protospacer region with caged nucleobases during solid-state RNA synthesis.<sup>25</sup> This approach achieves high activation rates and low background at the caged stage. However, it requires solid-state synthesis, which is not widely accessible, and each gRNA needs to be individually designed and optimized for its DNA target. UV light was also used to activate the gRNA.

Currently, no optically-modulated CRISPR editing system is capable of using multiple wavelengths of light to achieve multiplex editing, possibly due to the reliance of UV-activated photoprotecting groups. To develop a robust, versatile, photo-activated CRISPR-Cas9 editing system capable of using visible light we asked whether RNA-CLAMP could be adapted to control gRNA activity via site-specifically cross-linking the gRNA with photocleavable linkers. Cas9's endonuclease activity requires the binding of gRNA, following by the formation of the Cas9-gRNA ribonucleoprotein (RNP). After interacting with the protospacer adjacent motif near the target DNA, the RNP complex goes through a conformational change, which is critical to its nuclease activity.<sup>26–30</sup> Thus, we reasoned that cross-linking the internal loops of the gRNA would reduce the conformational flexibility of the Cas9-gRNA RNP, resulting in loss-of-function. Subsequent cleavage of the cross-linker

would remove the conformational restraint on the gRNA and activate gene editing. Here, we used RNA-CLAMP to cross-link two internal stem loops within the sgRNA. Upon clamping of the sgRNA, the Cas9-sgRNA RNP completely loses its DNA cleavage activity. Photocleavage of the crosslinker releases the gRNA and fully restores gene editing activity. Notably, cross-linkers that are responsive to different wavelengths of light can be used, allowing selection of the gene editing activation wavelength. We demonstrate multiplexed photo-activation of gene editing at two different genomic loci. The high efficiency of photo-activation enables spatiotemporal control, and we show that our technique allows gene editing within a single cell among a population of cells, which can be traced by time-lapse microscopy.

## RESULTS AND DISCUSSION

### Site-specific cross-linking of RNA by RNA-CLAMP

We previously developed a technique, RNA transglycosylation at guanosine (RNA-TAG), which enables site-specific and covalent conjugation of small molecule effectors, such as fluorophores, affinity tags, or translational regulators, onto an RNA of interest.<sup>31</sup> RNA-TAG utilizes a bacterial tRNA guanine transglycosylase (TGT) to exchange a guanine nucleobase within a specific 17-nucleotide RNA stem loop structure (Tag) with a modified analog of the natural substrate prequeosine1 (preQ1). Covalent modification is site-specific, robust, and irreversible, and RNA-TAG technology has been adapted to image cellular RNA in fixed cells, regulate mRNA translation, and study RNA-protein interactions.<sup>31–36</sup> RNA-TAG could, in principle, be used to cyclize RNA targets with synthetic linkers, achieved by introducing two recognition sites on a single RNA, and then creating an internal cross-link using a bivalent linker (Figure 1A). Crosslinking would likely affect the structure of the RNA, thus interfering with its normal function, whereas the cleavage of the cross-linker would release the RNA, resulting in restoration of function.

To determine whether RNA-TAG can be used for RNA intramolecular cross-linking (or clamping) we first verified that TGT enzymes accepted a bivalent linker (preQ1-PEG10-preQ1) and were able to dimerize small model RNA hairpins (Figure S1). To enable intramolecular cross-linking, an RNA substrate must have two TGT recognition motifs. Therefore, we designed a 74-nt long RNA molecule (RNA-1) with two Tag sequences and performed TGT enzymatic labeling using the preQ1-PEG10-preQ1 linker (Figure 1A). In order to distinguish between the various RNA products (Figure S2A), we designed an RNase-H digestion assay (Figure S2B), which specifically cleaves DNA-RNA hybrids.<sup>37–39</sup> Using a DNA oligo which hybridizes to the RNA, we observed that clamped RNA showed a single-band RNase-H digestion pattern, which is expected for an RNA that has been crosslinked intramolecularly. In contrast, all byproducts showed multi-band RNase-H digestion patterns (Figure S3). Thus, RNA-TAG can be used for site-specific and enzymatic cross-linking of two stem loops within an RNA of interest.

We asked whether RNA-CLAMP could be used to control CRISPR-Cas9 editing via cyclization of the sgRNA. The sgRNA is highly structured when in complex with dCas9 and target DNA, forming three stem loops and one tetraloop, with some of the stem loops being tolerant to mutations.<sup>26</sup> We screened the 17-nt Tag recognition sequence

(GCAGACUGUAAAUCUGC) at all 6 potential labeling sites within the sgRNA: insertion at the 5-end (sgRNA-1) or 3-end (sgRNA-6) and substituting the 17-nt Tag stem loop for either the tetra loop (sgRNA-2), stem loop 1 (sgRNA-3), stem loop 2 (sgRNA-4) or stem loop 3 (sgRNA-5) (Figure S4A). All the sgRNAs target the DYRK1A genome locus.<sup>40</sup> To screen for activity, we transiently transfected the sgRNAs into HEK-293 cells stably expressing Cas9 protein. Three days after transfection, genomic DNA was harvested and the sgRNA targeted region was amplified by PCR. Sanger sequencing results were analyzed using the ICE tool to determine the INDEL rate, which is representative of the gene editing efficiency of the sgRNA.<sup>41</sup> We found that sgRNA-1, sgRNA-3, and sgRNA-5 had significantly reduced activity (Figure S4B). For sgRNA-1, the 5-insertion of the Tag sequence might inhibit DNA strand invasion of the sgRNA, interfering with DNA cleavage. sgRNA-3 was less active, likely because the RNA three-way-junction structure formed near stem loop 1 plays a role in binding the Cas9 arginine-rich bridge helix and seems not to tolerate sequence modification.<sup>26</sup> sgRNA-5 likely has reduced activity because stem loop 3 interacts extensively with the Cas9 protein. However, sgRNA-2 and sgRNA-4 retained wild-type level activity, likely because the modified stem loops are solvent exposed and have been shown to tolerate sequence mutations.<sup>26</sup> Based on these findings, we constructed sgRNA-7, where two Tag sequences are inserted at both the tetraloop and stem loop 2 (Figure 2A). sgRNA-7 had wild-type level gene editing activity, making it the best candidate for cyclization using RNA CLAMP.

### sgRNA RNA-CLAMP modulates CRISPR-Cas9 editing

To determine the effect of intramolecular clamping on gene editing efficiency, we clamped sgRNA-7 using preQ1-PEG10-preQ1 and gel purified the clamped sgRNA-7. We observed a higher yield (78.5% conversion) of the cyclized clamped sgRNA after TGT labeling, compared to cross-linking of the RNA-1 (27.9% conversion, Figure S2A), likely due to the sgRNA being highly structured, wherein the tetra loop and the stem loop 2 are close to each other in space.<sup>26</sup> The clamped sgRNA-7 gave rise to 12.3% INDELS when used for gene editing in HEK-293 cells, compared to 80.7% INDELS when using the unmodified (linear) sgRNA-7, the loss in activity likely being due to clamping decreasing the conformational flexibility of the sgRNA.

To test this idea, we shortened the distance between the two cross-linked guanines to further rigidify the sgRNA, with the aim of completely silencing gene editing. TGT does not require the full 17-nt Tag sequence to label the RNA: A 7-nt (CUGUAAA) loop within a stable RNA stem structure (in this case, provided by the sgRNA backbone) is sufficient to promote TGT labeling. We constructed sgRNA-8, sgRNA-9, and sgRNA-10, which contained truncated stems of the Tag sequence (Figure S4A), thereby shortening the distance between the substituted guanines. We clamped sgRNA-8, sgRNA-9, and sgRNA-10 (Figure 2B), and tested their gene editing activity (Figure 2C). While clamped sgRNA-8 had 17.6% gene editing activity, compared to its unmodified form, clamped sgRNA-9 and sgRNA-10 had no detectable gene editing activity, demonstrating that reducing the distance between the two cross-linked guanine residues reduces or eliminates editing activity.

## Photo-activation of CRISPR-Cas9 gene editing

The sgRNA-9 maintained a wild-type level of gene editing activity in its unmodified form, and we thus used sgRNA-9 for our subsequent studies. To enable photo-activation of CRISPR-Cas9 gene editing, we synthesized the photocleavable small-molecule substrate, preQ1-DEACM-preQ1. Given TGT only recognizes the preQ1 moiety, and not the linker, we were able to choose from a variety of photosensitive linkers. The DEACM linker consists of a photoactive coumarin that can be cleaved by visible blue light, minimizing phototoxicity.<sup>42–45</sup> We clamped sgRNA-9 using the preQ1-DEACM-preQ1 substrate (79.4% conversion), purified the clamped sgRNA and characterized photocleavage (Figure S5A). Irradiation with a 456 nm LED light for 3 minutes completely cleaved the DEACM linker, transforming the clamped sgRNA to its linear form with no evidence of any background reactions (Figure S5B).

To test whether photocleavage of the crosslinker could activate the sgRNA in live mammalian cells, we delivered the linear, clamped, or pre-activated sgRNA-9 into a Cas9-expressing HEK293 cell line (Figure 3A). For pre-activation, clamped sgRNA-9 was irradiated with 456 nm light (LED) for 3 minutes prior to transfection. For live-cell photo-activation, sgRNA transfected cells were irradiated with 456 nm light for 3 minutes, 4 hours after transfection. Three days later, INDEL rates were analyzed to quantify gene editing efficiency. Pre-activation completely restored the activity of the clamped sgRNA to the wild-type level (Figure 3B). Live-cell photo-activation restored the clamped sgRNA-9's activity to 84.6% compared to wild-type. The slightly lower live-cell photo-activation might be due to degradation of the clamped sgRNA within the 4-hour transfection window. The clamped sgRNA completely blocked editing.

By using guide RNAs with different guide sequences, multiple genomic locations can be targeted at the same time using CRISPR-Cas9. Compared to light activation of Cas9 activity, light activation of the guide RNA should allow multiplexed photo-activated gene editing since RNA-CLAMP technology works with a range of photocleavable linkers. To test whether multiplexed photo-activation of gene editing is feasible, we synthesized a nitrobenzyl (NB) based photocleavable linker (the alkyne-NB-NHS ester building block is commercially available at BroadPharm, USA), preQ1-NB-preQ1, which can be cleaved by irradiation with 390 nm (UV) light (Figure 1B). The NB linker is not cleaved by the 456 nm light which is used to cleave the DEACM linker, whereas 390 nm light cleaves both linkers. This was because the DEACM photo-sensitive group also has maximal absorbance around 390 nm wavelength and the NB linker has nearly no absorbance at 456 nm wavelength. Thus, it is possible to control photocleavage and gene editing of two genes in a sequential and wavelength specific manner (Figure 3C). We used the preQ1-NB-preQ1 to clamp sgRNA-11, which targets the GRIN2B genome locus (20 bp targeting sequence: GGAGAACAGCACTCCGCTCT) (Figure 3C). sgRNA-11 has the same guide RNA backbone as the sgRNA-9. Clamped sgRNA-9 and clamped sgRNA-11 were transfected into Cas9-expressing HEK-293 cells. Cells were irradiated with either 456 nm light (3 minutes) or 390 nm LED light (30 seconds) to trigger the photo-activation of gene editing, as per previously established photo-activation protocols (Figure 3A). Gene editing efficiency was quantified by Sanger sequencing as INDEL%. Irradiation with the

456 nm light only triggered gene editing at the DYRK1A genome locus, while irradiation with the 390 nm wavelength of light triggered gene editing at both loci (Figure 3D). Thus, RNA-CLAMP photo-activated gene editing is compatible with different wavelengths of light enabling multiplexed photo-activation of editing.

To analyze the spatiotemporal resolution of our CRISPR-Cas9 photo-activation technology, we constructed a GFP reporter stable cell line which expresses GFP only when CRISPR-Cas9 gene editing occurs at the specific genome locus targeted by sgRNA-12 (sgRNA-12 targeting sequence: GTTCAGGGCTTGACCAACAC).<sup>46</sup> Once targeted gene editing takes place and an INDEL is formed as a result of the NHEJ DNA repair pathway, the out-of-frame GFP can be shifted in-frame, generating GFP signal as an indication of gene editing. The sgRNA-12 has the same sgRNA backbone as sgRNA-9. We used the preQ1-DEACM-preQ1 substrate to “clamp” sgRNA-12. In the absence of gene editing, the cells only expressed mCherry while edited cells expressed both mCherry and GFP. We delivered clamped sgRNA-12 into the reporter HEK-293 cells by transient transfection. 4 hours later, selected cells were irradiated with a 405 nm wavelength laser for 10 seconds (the DEACM linker has maximum absorbance around 400 nm wavelength), and imaged continuously. For example, a single cell was laser irradiated for 10 seconds to activate the clamped sgRNA (Figure 4). 15 hours later, the cell went through mitosis and GFP expression was observed in one of the daughter cells, indicating INDEL formation by CRISPR-Cas9 editing. We observed delayed GFP expression in gene edited cells (15 hours after photo-activation of gene editing) because it took cells an extended period of time to repair the Cas9 induced double-stranded break, form the frame-shifted INDEL, and transcribe and translate the GFP gene. This delay did not represent delayed photo-activation of gene editing. At 21.5 hours, GFP was continuously expressed in both of the daughter cells, and at 28.5 hours, one of the daughter cells went through mitosis, followed by mitosis in the other daughter cell, such that we ended up with a total of 4 cells expressing GFP as a result of single-cell light guided CRISPR-Cas9 gene editing.

### Clamped sgRNA forms Cas9-sgRNA RNPs and binds to target DNA

We asked whether clamped sgRNA maintains the capability to form the Cas9 RNP and bind to target DNA. We designed a 60 bp DNA substrate containing the sgRNA-9 target sequence with the NGG PAM, based on previous studies of sgRNA binding to Cas9 and target DNA.<sup>47</sup> We confirmed the DNA substrate bound to the Cas9-sgRNA RNP (Figure S8) using a non-targeting sgRNA-11 as the negative control. Formation of Cas9-sgRNA RNP was observed, using gel shift analysis, by mixing Cas9 protein with all three sgRNAs: linear sgRNA-9, clamped sgRNA-9, and linear sgRNA-11. We also observed the formation of the Cas9-sgRNA-DNA ternary complex by mixing Cas9 protein, the unmodified or clamped sgRNA-9, and the DNA substrate. However, the Cas9-sgRNA-DNA ternary complex was not observed for sgRNA-11 (the non-targeting sgRNA), demonstrating the specificity of the CRISPR-Cas9 system. These results suggest that although the RNA clamping completely quenches the DNA cleavage activity, the clamped RNP is still able to specifically recognize and bind to its DNA target. Further work will be required to decipher the precise mechanism by which clamping the sgRNA prevents Cas9 function.

## CONCLUSION

We have developed an RNA crosslinking approach, RNA-CLAMP, which allows site-specific and enzymatic cross-linking of two internal stem loops within an RNA of interest. By incorporating a photocleavable linker, the clamped RNA can be released by irradiation with a user-selected wavelength of light. Given the simplicity of the activation mechanism, RNA-CLAMP offers considerable flexibility through, for example, use of two photo-activatable crosslinkers that can be cleaved using different wavelengths of light. In principle, a variety of alternative photocleavable linkers can be used.<sup>48</sup> Multiplexed light activated gene editing should facilitate the study of complex gene networks with high spatiotemporal precision. Beyond photocleavable linkers, different conditionally cleavable linkers could also be used for clamping the RNA. For example, redox sensitive disulfide bonds, pH-sensitive linkers, and enzymatically cleavable peptides.<sup>49–52</sup> Furthermore, the RNA-CLAMP technique can also be used to intermolecularly cross-link two RNA molecules. The “RNA-CLAMP” technique, as applied in this work, was focused on the highly structured guide RNA of the CRISPR-Cas9 system. Future work will need to be done to validate the capability of “RNA-CLAMP” to cross-link longer RNAs, especially those without defined structures. However, we believe the versatility of our RNA-CLAMP technology will promote the development of a wide-range of biotechnologies to study RNA structures, RNA-RNA coupling, and RNA-protein interaction, where crosslinking of RNA would be valuable.<sup>8–10,53,54</sup>

We applied the RNA-CLAMP technique to the CRISPR-Cas9 sgRNA. By swapping the 4-nt sequence (GAAA) within the sgRNA tetra loop and stem loop 2 for the 7-nt TGT recognition motif (CUGUAAA), we were able to site-specifically cross-link the two guanine residues within the TGT recognition motifs, resulting in the Cas9-sgRNA RNP complex completely losing its DNA cleavage activity while maintaining the ability to bind its DNA target. Live-cell photo-irradiation triggered cleavage of the crosslinker and activated CRISPR-Cas9 gene editing. This photo-activated gene editing platform has nondetectable gene editing background at the caged stage and a high cellular activation rate (84.6%). Photo-activation also offers high spatiotemporal precision. We were able to photo-activate CRISPR-Cas9 editing within a single cell in a population of cells. Furthermore, by using photocleavable linkers which are responsive to different wavelengths of light, we achieved multiplexed photo-activation of gene editing. We are confident our approach will lead to future development of photo-activated gene editing technologies capable of deciphering complex gene networks, as well as stimuli responsive CRISPR-based gene therapies.

## EXPERIMENTAL SECTION

### RNA labeling using the RNA-CLAMP technology

**In vitro transcription of sgRNA**—Each IVT reaction was set up with 50 nM of linearized DNA template, 5 mM of each ATP, CTP, UTP, 9 mM of GTP (NEB, Ipswich, MA), 0.004 unit/ $\mu\text{L}$  of thermostable inorganic pyrophosphatase (NEB, Ipswich, MA), 0.25  $\mu\text{g}/\mu\text{L}$  T7 RNA polymerase, 0.05% Triton X-100 (Sigma, St. Louis, MO) and 1 unit/ $\mu\text{L}$  RNase Inhibitor, Murine (NEB, Ipswich, MA). The IVT reaction was carried out at 37 °C for 4 hours to allow for sufficient RNA synthesis. To remove DNA template, 2  $\mu\text{L}$  of 100

mM CaCl<sub>2</sub> and 20 units of Turbo DNase (Life Technologies, Carlsbad, CA) were added to the mixture and incubated at 37 °C for 1 hour. The mixture was then centrifuged at 10,000 RCF for 5 minutes at room temperature to pellet any remaining magnesium pyrophosphate. The supernatant was resuspended in 50  $\mu$ L RNase free water, followed by 12% denaturing PAGE purification. Purified IVT products were stored at -80°C until used.

**Dimerization of the 17-nt Tag RNA oligo by RNA-CLAMP**—17-nt RNA Tag oligo (GCAGACUGUAAAUCUGC) was purchased from IDT. TGT labeling reaction was assembled with the following components in 1X TGT reaction buffer: 10  $\mu$ M of 17-nt RNA oligo, 5  $\mu$ M of TGT enzyme, 5  $\mu$ M of small-molecule substrate (preQ1-PEG10-preQ1, Figure S1A), and 5 mM DTT. The reaction mixture was incubated at 37 °C for 4 hours. 1  $\mu$ L of proteinase K was added into reaction mixture and incubated at 37°C for 30 minutes to terminate the labeling reaction. The reaction was analyzed on 18% denaturing PAGE (Figure S1B). In Figure S1B, we can see that after the TGT labeling reaction, two new RNA products were produced. The top RNA band is the dimerized 17-nt Tag oligo. The middle band is the singly labeled Tag oligo. This experiment demonstrated the capability of the TGT enzyme to form a covalent bond between two RNA hairpins and builds the foundation for our RNA-CLAMP technology.

**Intramolecular cross-link of the RNA**—The in vitro transcription reaction was performed following previous established protocols.<sup>31</sup> PAGE gel purified RNA-1 was subjected to TGT labeling reaction using the preQ1-PEG10-preQ1 small-molecule substrate. TGT labeling reaction was assembled with the following components in 1X TGT reaction buffer: 1  $\mu$ M of RNA-1, 2  $\mu$ M of TGT enzyme, 1  $\mu$ M of small-molecule substrate (preQ1-PEG10-preQ1, Figure S1A), 1 unit/ $\mu$ L of Super RNase Inhibitor (Invitrogen, catalog number AM2694), and 5 mM DTT. The reaction mixture was incubated at 37 °C for 4 hours. Next, 1  $\mu$ L of proteinase K was added into the reaction mixture and incubated at 37°C for 30 minutes to terminate the labeling reaction and get rid of potential RNase contamination. Note: adding the small-molecule substrate last should promote higher ‘clamping’ conversion. The reason is that the TGT enzyme forms a covalent bound with the RNA substrate, resulting in a TGT-RNA intermediate. Adding the small-molecule substrate last ensured that two TGT molecules were covalently tethered to the RNA. In this manner, intermolecular cross-linking of RNA can be reduced. The crude TGT labeling products were analyzed by 7% denaturing TBE PAGE (Figure S2A). As shown in Figure S2A, we observed multiple RNA products. First, we observed unlabeled RNA starting material, shown as the bottom band with the same migration distance as Line 1. We also observed RNA degradation shown as smear bands below the RNA starting material. We hypothesize that, apart from the desired ‘clamped’ RNA product, the TGT labeling reaction should at least generate two kinds of by-products: by-product 1 was generated by attaching one small-molecule substrate at each Tag sequence without forming intermolecular or intramolecular cross-linking; by-product 2 was formed through intermolecular cross-linking, which were shown as multiple top bands in Line 2.

To distinguish between multiple RNA products after the TGT reaction, we designed an RNase-H digestion assay (Figure S2C). RNase-H only digests RNA-DNA hybrids. We

designed a DNA oligo which was complementary to the internal sequence of RNA-1 and use RNase-H to specifically cut the internal sequence of RNA-1. As illustrated in Figure S2C, after the RNase-H digestion (DNA oligo used for the RNase-H digestion assay on RNA-1: CCAGCACACTGGCGGCCG), linear RNA products would generate two RNA fragments whereas the ‘clamped’ RNA product would only generate one RNA digestion product. We separated the product bands observed on Figure S2A (Line 2) and ran each RNA product through the RNase-H digestion assay (Figure S3). As expected, both the RNA byproduct-1 and byproduct-2 generated two or multiple bands after the RNase-H digestion assay. Only the ‘clamped’ RNA product generated one single band after the RNase-H digestion assay. Therefore, we verified that TGT can successfully form an intramolecular cross-link (or ‘clamp’) on the RNA of interest using the preQ1-PEG10-preQ1 small-molecule substrate.

### Intramolecular cross-link of the sgRNA by RNA-CLAMP

To ‘clamp’ the sgRNA-9, 1  $\mu\text{M}$  of sgRNA transcript, 1  $\mu\text{M}$  of TGT enzyme, 1  $\mu\text{M}$  of small-molecule substrate, 5 mM of DTT, 1 unit/ $\mu\text{L}$  of RNase Inhibitor was assembled in 1X TGT buffer. The reaction mixture was incubated at 37°C for 4 hours, followed by the addition of 1  $\mu\text{L}$  of proteinase K. The crude labeling products were analyzed by 12% denaturing TBE-PAGE (Figure S5A). As shown in Figure S5A, the conversion rate to the ‘clamped’ sgRNA was 79.4%, which is much higher than the conversion rate of the RNA-1. We reasoned that this was due to the stable ternary structure of the sgRNA. The first Tag sequence was located at the tetra-loop of the sgRNA and the second Tag sequence was located at the stem loop 2 of the sgRNA. These two loops are well-structured and close to each other, promoting higher intramolecular cross-linking conversion. To get rid of undesired RNA product and reduce background gene editing activity, ‘clamped’ sgRNA-9 was purified by denaturing TBE-PAGE. The purified ‘clamped’ sgRNA-9 was shown as a single band on a 12% denaturing PAGE gel (Figure S5B). To uncage the ‘clamped’ sgRNA-9, a 456 nm LED light (50W max) was used to irradiate the ‘clamped’ sgRNA in water for 3 minutes. LED irradiation completely photo-cleaved the DEACM linker, transforming the ‘clamped’ sgRNA to its linear form (Figure S5B).

Similarly, we performed RNA-CLAMP reaction on sgRNA-11 using the preQ1-NB-preQ1 small molecule substrate. As shown in Figure S6, the ‘clamped’ sgRNA-11 can be completely photo-uncaged by irradiation with a 390 nm LED light (52W max) for 30 seconds. As a control experiment, we irradiated the ‘clamped’ sgRNA-11 using the 456 nm LED light for 3 minutes. Only minimal photo-cleavage of the NB linker was observed (0.09%), demonstrating that the NB linker can be efficiently cleaved by a 390 nm LED, but not a 456 nm LED.

### Surrogate GFP reporter for the detection of gene editing

The surrogate EGFP reported was adopted from a previously reported method.<sup>46</sup> In brief, an mCherry transgene is constitutively expressed by a CMV promoter, whereas the expression of downstream GFP genes are disrupted by an in-frame stop codon as well as a frame shift (+1 or +2 shift). Without INDEL formation, the cell will express mCherry but not GFP. However, when an INDEL is formed by CRISPR-Cas9 mediated gene editing and

the cellular NHEJ pathway, the frame shift of the downstream GFP gene can be corrected, resulting in GFP expression.

### **In vitro Cas9-sgRNA-DNA binding assay**

We investigated the binding of the unmodified or ‘clamped’ sgRNA with the Cas9 protein (NEB, catalog number M0646T) in vitro. First, we designed a double-stranded 60 bp DNA substrate which contains the sgRNA-9 target sequence with the required NGG PAM. We used sgRNA-11 as the negative control non-targeting sgRNA, since sgRNA-11 did not target the 60 bp DNA substrate. To test the binding the sgRNA and the 60 bp DNA substrate in vitro, 200 nM of Cas9 enzyme and 200 nM of sgRNA were incubated in 1X NEB buffer 3.1 for 15 minutes at room temperature. Next, 20 nM of DNA substrate was added into the pre-formed Cas9-sgRNA RNP and incubated at 37°C for 90 seconds. After the incubation, the reaction mixture was immediately placed on ice with the addition of 50% reaction volume of 50% glycerol to stop the reaction (Note: it is important to quench the reaction as quickly as possible.). Finally, the reaction was analyzed on 5% native TBE-PAGE (Figure S8). In Figure S8, lane 1 to lane 3 are the loading control of the sgRNA. The unmodified sgRNA-9 and sgRNA-11 were shown as multiple bands in the native TBE gel due to their secondary/ternary structures. Interestingly, the ‘clamped’ sgRNA-9 was shown as a single major band on the native gel. We reasoned it was because the intramolecular clamping rigidified the structure of the sgRNA. The formation of the sgRNA-9 Cas9 RNP was detected in lane 4. The formation of the Cas9-sgRNA-DNA ternary complex was only detected in lane 5 (unmodified sgRNA-9) and lane 6 (‘clamped’ sgRNA-9), but not in lane 7 (non-targeting sgRNA-11), demonstrating that the ‘clamped’ sgRNA-9 was also able to bind to the Cas9 as well as the target DNA in vitro.

### **Supplementary Material**

Refer to Web version on PubMed Central for supplementary material.

### **Acknowledgement**

We thank Life Science Editors for editorial assistance and advice. The project or effort depicted was sponsored by the Defense Advanced Research Projects Agency Biological Technologies Office (BTO) Safe Genes Program under Contract Number HR0011-18-2-0039 and the National Institutes of Health under grant R01 GM123285. The content of the information does not necessarily reflect the position or the policy of the government, and no official endorsement should be inferred.

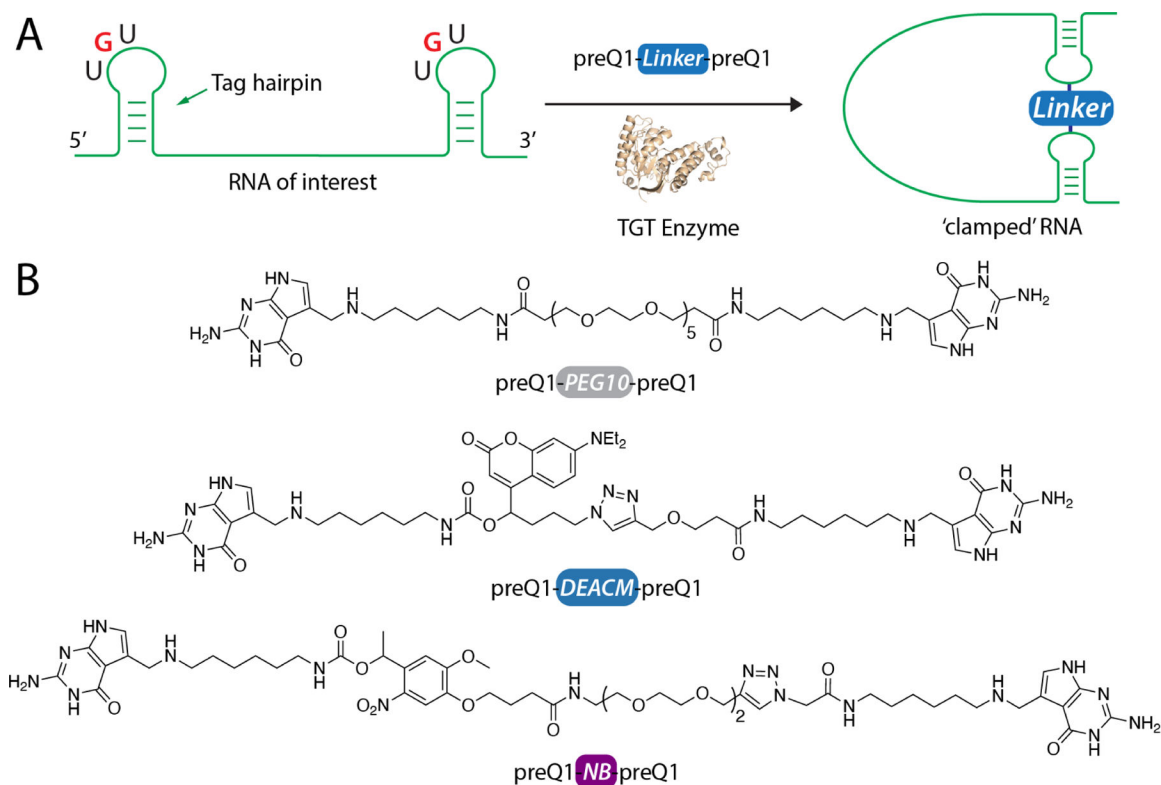
### **References**

- (1). Armitage BA Imaging of RNA in live cells. *Current opinion in chemical biology* 2011, 15, 806–812. [PubMed: 22055496]
- (2). Alexander SC; Devaraj NK Developing a fluorescent toolbox to shed light on the mysteries of RNA. *Biochemistry* 2017, 56, 5185–5193. [PubMed: 28671838]
- (3). Schulz D; Rentmeister A Current approaches for RNA labeling in vitro and in cells based on click reactions. *ChemBioChem* 2014, 15, 2342–2347. [PubMed: 25224574]
- (4). Dolgoshina EV; Unrau PJ Fluorophore-binding RNA aptamers and their applications. *Wiley Interdisciplinary Reviews: RNA* 2016, 7, 843–851. [PubMed: 27501452]
- (5). Velema WA; Park HS; Kadina A; Orbai L; Kool ET Trapping transient RNA complexes by chemically reversible acylation. *Angewandte Chemie* 2020, 132, 22201–22206.

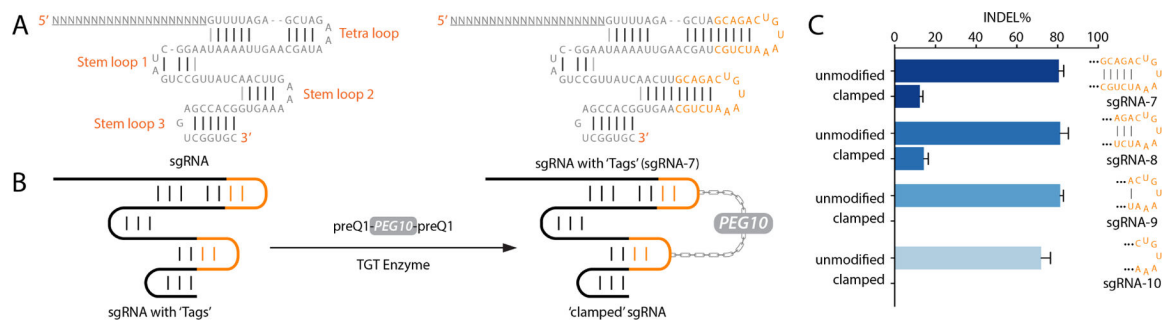
- (6). Velema WA; Kool ET The chemistry and applications of RNA 2-OH acylation. *Nature Reviews Chemistry* 2020, 4, 22–37.
- (7). Holstein JM; Rentmeister A Current covalent modification methods for detecting RNA in fixed and living cells. *Methods* 2016, 98, 18–25. [PubMed: 26615954]
- (8). Kaewsapsak P; Shechner DM; Mallard W; Rinn JL; Ting AY Live-cell mapping of organelle-associated RNAs via proximity biotinylation combined with protein-RNA crosslinking. *Elife* 2017, 6, e29224. [PubMed: 29239719]
- (9). Dorn G; Leitner A; Boudet J; Campagne S; von Schroetter C; Moursy A; Aebersold R; Allain FH Structural modeling of protein–RNA complexes using crosslinking of segmentally isotope-labeled RNA and MS/MS. *Nature methods* 2017, 14, 487–490. [PubMed: 28346450]
- (10). Hentze MW; Castello A; Schwarzl T; Preiss T A brave new world of RNA-binding proteins. *Nature reviews Molecular cell biology* 2018, 19, 327–341. [PubMed: 29339797]
- (11). Suresh BM; Li W; Zhang P; Wang KW; Yildirim I; Parker CG; Disney MD A general fragment-based approach to identify and optimize bioactive ligands targeting RNA. *Proceedings of the National Academy of Sciences* 2020, 117, 33197–33203.
- (12). Mukherjee H; Blain JC; Vandivier LE; Chin DN; Friedman JE; Liu F; Maillet A; Fang C; Kaplan JB; Li J, et al. PEARL-seq: a photoaffinity platform for the analysis of small molecule-RNA interactions. *ACS Chemical Biology* 2020, 15, 2374–2381. [PubMed: 32804474]
- (13). Velagapudi SP; Li Y; Disney MD A cross-linking approach to map small molecule-RNA binding sites in cells. *Bioorganic & medicinal chemistry letters* 2019, 29, 1532–1536. [PubMed: 30987892]
- (14). Velagapudi SP; Cameron MD; Haga CL; Rosenberg LH; Lafitte M; Duckett DR; Phinney DG; Disney MD Design of a small molecule against an oncogenic noncoding RNA. *Proceedings of the National Academy of Sciences* 2016, 113, 5898–5903.
- (15). Dow LE; Fisher J; O’rourke KP; Muley A; Kasthuber ER; Livshits G; Tschaharganeh DF; Succi ND; Lowe SW Inducible in vivo genome editing with CRISPR-Cas9. *Nature biotechnology* 2015, 33, 390–394.
- (16). Zetsche B; Volz SE; Zhang F A split-Cas9 architecture for inducible genome editing and transcription modulation. *Nature biotechnology* 2015, 33, 139–142.
- (17). Kim S; Kim D; Cho SW; Kim J; Kim J-S Highly efficient RNA-guided genome editing in human cells via delivery of purified Cas9 ribonucleoproteins. *Genome research* 2014, 24, 1012–1019. [PubMed: 24696461]
- (18). Zuris JA; Thompson DB; Shu Y; Guilinger JP; Bessen JL; Hu JH; Maeder ML; Joung JK; Chen Z-Y; Liu DR Cationic lipid-mediated delivery of proteins enables efficient protein-based genome editing in vitro and in vivo. *Nature biotechnology* 2015, 33, 73–80.
- (19). Ramakrishna S; Dad A-BK; Beloor J; Gopalappa R; Lee S-K; Kim H Gene disruption by cell-penetrating peptide-mediated delivery of Cas9 protein and guide RNA. *Genome research* 2014, 24, 1020–1027. [PubMed: 24696462]
- (20). Hemphill J; Borchardt EK; Brown K; Asokan A; Deiters A Optical control of CRISPR/Cas9 gene editing. *Journal of the American Chemical Society* 2015, 137, 5642–5645. [PubMed: 25905628]
- (21). Nihongaki Y; Kawano F; Nakajima T; Sato M Photoactivatable CRISPR-Cas9 for optogenetic genome editing. *Nature biotechnology* 2015, 33, 755–760.
- (22). Jain PK; Ramanan V; Schepers AG; Dalvie NS; Panda A; Fleming HE; Bhatia SN Development of Light-Activated CRISPR Using Guide RNAs with Photo-cleavable Protectors. *Angewandte Chemie International Edition* 2016, 55, 12440–12444. [PubMed: 27554600]
- (23). Gu C; Xiao L; Shang J; Xu X; He L; Xiang Y Chemical synthesis of stimuli-responsive guide RNA for conditional control of CRISPR-Cas9 gene editing. *Chemical Science* 2021, 12, 9934–9945. [PubMed: 34377390]
- (24). Wang S; Wei L; Wang J-Q; Ji H; Xiong W; Liu J; Yin P; Tian T; Zhou X Light-Driven Activation of RNA-Guided Nucleic Acid Cleavage. *ACS chemical biology* 2020, 15, 1455–1463. [PubMed: 32378871]
- (25). Zhou W; Brown W; Bardhan A; Delaney M; Ilk AS; Rauen RR; Kahn SI; Tsang M; Deiters A Spatiotemporal control of CRISPR/Cas9 function in cells and zebrafish using light-activated guide RNA. *Angewandte Chemie* 2020, 132, 9083–9088.

- (26). Nishimasu H; Ran FA; Hsu PD; Konermann S; Shehata SI; Dohmae N; Ishitani R; Zhang F; Nureki O Crystal structure of Cas9 in complex with guide RNA and target DNA. *Cell* 2014, 156, 935–949. [PubMed: 24529477]
- (27). Jiang F; Doudna JA CRISPR–Cas9 structures and mechanisms. *Annual review of biophysics* 2017, 46, 505–529.
- (28). Doudna JA; Charpentier E The new frontier of genome engineering with CRISPR-Cas9. *Science* 2014, 346, 1077.
- (29). Hsu PD; Lander ES; Zhang F Development and applications of CRISPR-Cas9 for genome engineering. *Cell* 2014, 157, 1262–1278. [PubMed: 24906146]
- (30). Harrington LB; Doxzen KW; Ma E; Liu J-J; Knott GJ; Edraki A; Garcia B; Amrani N; Chen JS; Cofsky JC, et al. A broad-spectrum inhibitor of CRISPR-Cas9. *Cell* 2017, 170, 1224–1233. [PubMed: 28844692]
- (31). Alexander SC; Busby KN; Cole CM; Zhou CY; Devaraj NK Site-Specific covalent labeling of RNA by enzymatic transglycosylation. *Journal of the American Chemical Society* 2015, 137, 12756–12759. [PubMed: 26393285]
- (32). Ehret F; Zhou CY; Alexander SC; Zhang D; Devaraj NK Site-specific covalent conjugation of modified mRNA by tRNA guanine transglycosylase. *Molecular pharmaceutics* 2017, 15, 737–742. [PubMed: 28749687]
- (33). Zhou CY; Alexander SC; Devaraj NK Fluorescent turn-on probes for wash-free mRNA imaging via covalent site-specific enzymatic labeling. *Chemical science* 2017, 8, 7169–7173. [PubMed: 29081948]
- (34). Zhang D; Zhou CY; Busby KN; Alexander SC; Devaraj NK Light-activated control of translation by enzymatic covalent mRNA Labeling. *Angewandte Chemie* 2018, 130, 2872–2876.
- (35). Zhang D; Jin S; Piao X; Devaraj NK Multiplexed photoactivation of mRNA with single-Cell resolution. *ACS chemical biology* 2020, 15, 1773–1779. [PubMed: 32484653]
- (36). Busby KN; Fulzele A; Zhang D; Bennett EJ; Devaraj NK Enzymatic RNA Biotinylation for Affinity Purification and Identification of RNA–Protein Interactions. *ACS Chemical Biology* 2020, 15, 2247–2258. [PubMed: 32706237]
- (37). Nakamura H; Oda Y; Iwai S; Inoue H; Ohtsuka E; Kanaya S; Kimura S; Katsuda C; Katayanagi K; Morikawa K How does RNase H recognize a DNA. RNA hybrid? *Proceedings of the National Academy of Sciences* 1991, 88, 11535–11539.
- (38). Klumpp K; Hang JQ; Rajendran S; Yang Y; Derosier A; Wong Kai In P; Overton H; Parkes KE; Cammack N; Martin JA Two-metal ion mechanism of RNA cleavage by HIV RNase H and mechanism-based design of selective HIV RNase H inhibitors. *Nucleic acids research* 2003, 31, 6852–6859. [PubMed: 14627818]
- (39). Nowotny M; Gaidamakov SA; Crouch RJ; Yang W Crystal structures of RNase H bound to an RNA/DNA hybrid: substrate specificity and metal-dependent catalysis. *Cell* 2005, 121, 1005–1016. [PubMed: 15989951]
- (40). Ran FA; Hsu PD; Wright J; Agarwala V; Scott DA; Zhang F Genome engineering using the CRISPR-Cas9 system. *Nature protocols* 2013, 8, 2281–2308. [PubMed: 24157548]
- (41). Conant D; Hsiao T; Rossi N; Oki J; Maures T; Waite K; Yang J; Joshi S; Kelso R; Holden K; Enzmann BL; Stoner R Inference of CRISPR Edits from Sanger Trace Data. *The CRISPR Journal* 2022, 5, 123–130. [PubMed: 35119294]
- (42). Pinheiro AV; Baptista P; Lima JC Light activation of transcription: photocaging of nucleotides for control over RNA polymerization. *Nucleic acids research* 2008, 36, e90–e90. [PubMed: 18586819]
- (43). Hagen V; Bendig J; Frings S; Eckardt T; Helm S; Reuter D; Kaupp UB Highly efficient and ultrafast phototriggers for cAMP and cGMP by using long-wavelength UV/VIS-activation. *Angewandte Chemie International Edition* 2001, 40, 1045–1048. [PubMed: 11268067]
- (44). Hagen V; Frings S; Wiesner B; Helm S; Kaupp UB; Bendig J [7-(Dialkylamino) coumarin-4-yl] methyl-Caged Compounds as Ultrafast and Effective Long-Wavelength Phototriggers of 8Bromo-Substituted Cyclic Nucleotides. *ChemBioChem* 2003, 4, 434–442. [PubMed: 12740815]

- (45). Goguen BN; Aemissegger A; Imperiali B Sequential activation and deactivation of protein function using spectrally differentiated caged phosphoamino acids. *Journal of the American Chemical Society* 2011, 133, 11038–11041. [PubMed: 21692531]
- (46). Kim H; Um E; Cho S-R; Jung C; Kim H; Kim J-S Surrogate reporters for enrichment of cells with nuclease-induced mutations. *Nature methods* 2011, 8, 941–943. [PubMed: 21983922]
- (47). Wu X; Scott DA; Kriz AJ; Chiu AC; Hsu PD; Dadon DB; Cheng AW; Trevino AE; Konermann S; Chen S, et al. Genome-wide binding of the CRISPR endonuclease Cas9 in mammalian cells. *Nature biotechnology* 2014, 32, 670–676.
- (48). Luciano MP; Nourian S; Gorka AP; Nani RR; Nagaya T; Kobayashi H; Schnermann MJ A near-infrared light-mediated cleavable linker strategy using the heptamethine cyanine chromophore. *Methods in Enzymology* 2020, 641, 245–275. [PubMed: 32713525]
- (49). Antelmann H; Helmann JD Thiol-based redox switches and gene regulation. *Antioxidants & redox signaling* 2011, 14, 1049–1063. [PubMed: 20626317]
- (50). Choy CJ; Geruntho JJ; Davis AL; Berkman CE Tunable pH-sensitive linker for controlled release. *Bioconjugate chemistry* 2016, 27, 824–830. [PubMed: 26886721]
- (51). Leriche G; Chisholm L; Wagner A Cleavable linkers in chemical biology. *Bioorganic & medicinal chemistry* 2012, 20, 571–582. [PubMed: 21880494]
- (52). Bargh JD; Isidro-Llobet A; Parker JS; Spring DR Cleavable linkers in antibody–drug conjugates. *Chemical Society Reviews* 2019, 48, 4361–4374. [PubMed: 31294429]
- (53). Juzumiene D; Shapkina T; Kirillov S; Wollenzien P Short-range RNA-RNA crosslinking methods to determine rRNA structure and interactions. *Methods* 2001, 25, 333–343. [PubMed: 11860287]
- (54). Harris ME; Christian EL RNA crosslinking methods. *Methods in enzymology* 2009, 468, 127–146. [PubMed: 20946768]

**Figure 1:**

The RNA-CLAMP technique. B) Chemical structure of bivalent TGT enzymatic small-molecule substrates preQ1-PEG10-preQ1, preQ1-DEACM-preQ1 and preQ1-NB-preQ1. The preQ1-PEG10-preQ1 substrate is not photosensitive. The [7-(diethylamino)coumarin-4-yl]-methyl (DEACM) linker is photocleaved by irradiation with 405–456 nm light. The nitrobenzyl based (NB) linker is photocleaved by irradiation with 356–390 nm light.

**Figure 2:**

sgRNA crosslinking by RNA-CLAMP. A) Sequence of the sgRNA. The sgRNA has four stem loops, which can be swapped with the Tag sequences to facilitate TGT enzymatic labeling. We replaced the tetra loop and the stem loop 2 of the sgRNA to form sgRNA-7. Modification did not compromise gene editing activity. B) sgRNA with 'Tags' can be intramolecularly crosslinked by RNA-CLAMP. In this example, the preQ1-PEG10-preQ1 small-molecule substrate was used as the cross-linker to form the 'clamped' sgRNA. C) Gene editing efficiency of truncated sgRNA-8 to sgRNA-10 compared to nontruncated sgRNA-7. Truncating 2 or 4 base pairs within the 'Tag' sequences of the sgRNA had little effect on gene editing efficiency, as shown in the figure that the unmodified sgRNA-7 (no truncation), sgRNA-8 (truncate 2 base pairs), and sgRNA-9 (truncate 4 base pairs) has similar gene editing activity. However, truncating 4 or 5 base pairs within the 'Tag' sequences of the sgRNA completely deactivated gene editing when the sgRNAs were at the 'clamped' form. As shown in the figure, the 'clamped' sgRNA-9 (truncate 4 base pairs) and sgRNA-10 (truncate 5 base pairs) had no detectable gene editing activity. Error bar represented standard deviation.

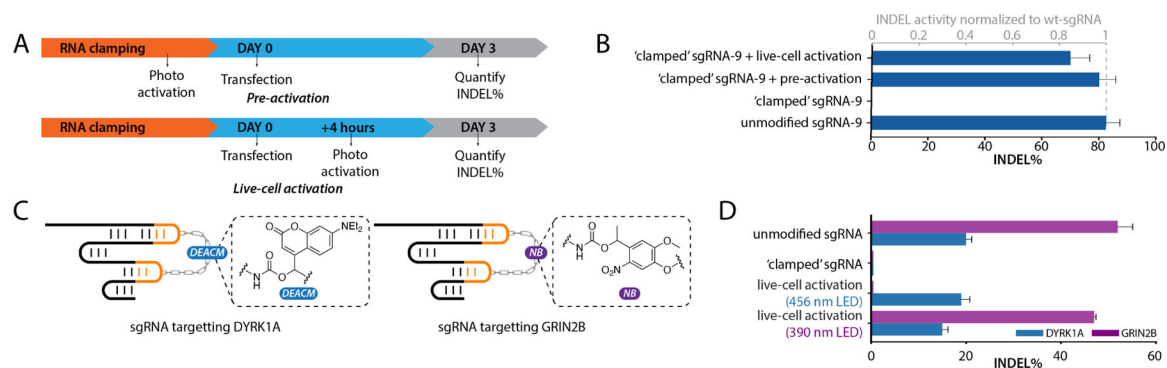
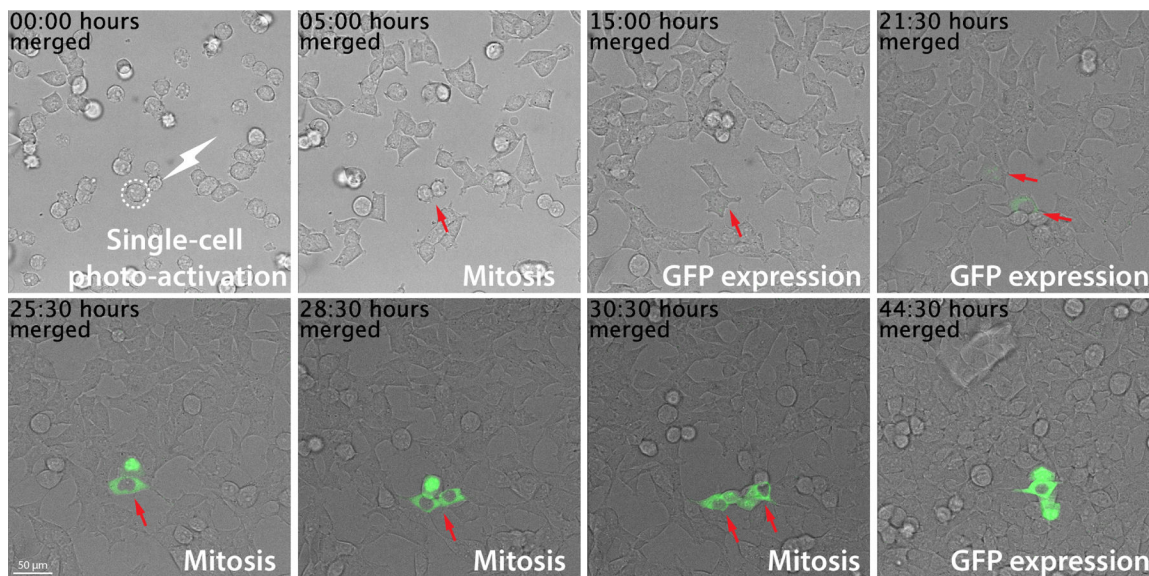
**Figure 3:**

Photo-activation of CRISPR-Cas9 gene editing. A) Experimental design of pre-activation and live-cell photo-activation of the 'clamped' sgRNA. For pre-activation, the clamped sgRNA was uncaged prior to transfection. For live-cell activation, LED light was directly applied to HEK-293 cells 4 hours after the transfection event. B) Photo-irradiation restored CRISPR-Cas9 gene editing. Pre-activation almost completely restored gene editing activity of 'clamped' sgRNA-9 (97% compared to unmodified sgRNA-9). Live-cell activation also restored gene editing activity of 'clamped' sgRNA (85% compared to unmodified sgRNA-9). C) For multiplexed photo-activation of gene editing, the preQ1-DEACM-preQ1 substrate was used to clamp a sgRNA targeting the DYRK1A genomic site, and the preQ1-NB-preQ1 substrate was used to clamp a sgRNA targeting the GRIN2B genomic site. D) Multiplexed photo-activation of gene editing. Either 456 nm or 390 nm LED light was used to photo-activate gene editing. The 456 nm LED light only cleaved the DEACM photosensitive linker, activating the sgRNA targeting the DYRK1A site. The 390 nm LED light cleaved both the DEACM and the NB photosensitive linkers, therefore activating gene editing at both genome loci.



**Figure 4:** Single-cell photo-activation of CRISPR-Cas9 gene editing using a GFP reporter stable cell line. At the 0 hour time point, one single cell was irradiated with a 405 nm laser for 10 seconds. After 5 hours, the laser irradiated cell went through mitosis (red arrow). After 15 hours, one daughter cell started expressing GFP. The other daughter cell expressed GFP after 21.5 hours. Cells were continuously imaged for 44.5 hours to observe GFP expression. Notably, only the laser irradiated cell and its daughter cells expressed GFP, but not the surrounding cells, demonstrating single-cell resolution of photo-activated gene editing. The expressed GFP localized to the cytoplasm, which was expected since the GFP protein did not contain any subcellular targeting moieties such as a nuclear localization sequence. Scale bar=50 $\mu$ m.